JOURNAL OF PROPULSION AND POWER
Vol. 24, No. 2, March–April 2008

Wave Reverberations in Multitube Pulse Detonation Engines

Houshang B. Ebrahimi*
Aerospace Testing Alliance,
Arnold Air Force Base, Tennessee 37389
and
Charles L. Merkle†
Purdue University, West Lafayette, Indiana 46905

DOI: 10.2514/1.32162

Internal wave reverberation processes in multiple-tube, pulsed detonation engines are considered. The study is based on a two-dimensional analysis of dual- and triple-detonation tubes exhausting through a common nozzle. Computations are first performed for a series of dual-tube configurations in which the intertube geometry is varied parametrically. Similar computations are then performed for three-tube configurations. The results indicate that when a detonation exits one tube, the details of the geometrical interconnection between tubes can change the magnitude of the pressure spike produced in an adjacent tube by nearly an order of magnitude. Controlling the crosstalk between adjacent tubes represents an important prerequisite for understanding propellant fill procedures and shock wave propagation in multitube devices.

I. Introduction

MAJOR advances in the operation and understanding of pulsed detonation tubes have been realized in the past decade. Although concepts using detonations in propulsive applications have been pursued for 50 years [1], a recurring initial difficulty was an inability to realize the theoretical detonation pressure rise [2,3]. Improved understanding of detonation initiation has removed this barrier, and repeatable detonations that match the theoretical pressure rise are now routinely achieved [4–8]. Specific impulse measurements by ballistic pendulum [7], thrust balance [6], and integrated pressure measurements [4] have also rectified earlier disagreements [9,10] on the performance potential of pulse detonation engines (PDEs). Current attention in PDE experiments is focused on issues such as flow control [11], the effects of heat loss [12], detonation initiation in sprays and the minimization of initiation energies [13], the effects of ambient pressure on performance [14], and multiple-tube effects [15].

A variety of analytical approaches has also been used to model PDE operation. Quasi-steady cycle analyses [16,17] offer direct performance comparisons with conventional propulsive devices and indicate that the efficiency of the PDE modestly exceeds that of a constant-volume combustion cycle. Unsteady, semi-analytical models such as those by Talley and Coy [18] and Wintenberger et al. [19], who follow an approach philosophically similar to that used by Zitoun and Desbourdes [4], provide a capability for rapid design analyses. Talley and Coy couple a constant-volume combustion process with a lumped-parameter blowdown analysis, whereas Wintenberger et al. use Taylor self-similar theory from detonation analysis in conjunction with numerical results and empirical measurements to approximate the blowdown process in closed fashion. In general, these models compare well with data from single-pulse experiments. The Wintenberger model has been extended to include effects of fill velocity [20] and ambient pressure [14] among other parameters, giving it reasonably comprehensive capabilities for discerning parametric trends in performance. Wintenberger and Shepherd [21] have also dealt with the subtleties concerning the propulsive efficiency in steady vs unsteady detonations and shown that, whereas unsteady detonations generate smaller entropy rise than deflagrations, steady detonations generate larger entropy rise than constant-pressure combustion. These findings are in agreement with early work by Zel'dovich, which has recently been republished [22]. One- and two-dimensional unsteady numerical models have also been used to address a variety of issues in PDE applications. Cambier and Tegner [23] discuss issues related to optimization of PDE performance, including a brief assessment of the effects of nozzles, and show that the energy used for initiating the numerical detonations can contribute appreciably to the indicated performance. Li and Kailasanath [24] deal with the performance issues associated with filling only part of the detonation tube with fuel, a procedure that improves the specific impulse but decreases the net impulse, providing an interesting tradeoff for design applications. Fan and Lu [25] indicate that chambers of variable cross sections offer potential for higher performance, whereas both Morris [26] and He and Karagozian [27] find that a converging–diverging nozzle improves performance, and He and Karagozian [27] conclude that a converging nozzle can decrease performance. Perkins and Sung [28] use numerical simulations to address the effects of incomplete mixing and show that modest fuel/air gradients in either the axial or radial directions have minor effects on performance.

Wu et al. [29] and Ma et al. [30] present the most complete system model for PDEs, which includes an inlet, combustor, and nozzle for a supersonic application. Their results indicate that a converging–diverging nozzle is necessary to make a PDE competitive with an ideal ramjet. The absence of a choked throat to prevent total pressure loss between the inlet and the detonation tube results in performance that is much lower than that of the ramjet. They also note [30] that multipulse operations can have important differences from single-pulse analyses that have been used in most earlier works. Similar observations on the significance of multipulse operations were noted earlier by Ebrahimi et al. [31].

All the studies delineated in the preceding (with the exception of [15]) have dealt with isolated detonation tubes. Most PDE applications, however, envision combining multiple detonation tubes into a single engine to mitigate the relatively low time-averaged

Received 15 May 2007; accepted for publication 15 May 2007.

*Engineer/Scientist, Propulsion Technology, Arnold Engineering Development Center, 1099 Avenue C, Mail Stop 9013; currently at Raytheon Missile Systems, 1151 East Hermans Road, Mail Stop TU/805/L5, Tucson, AZ 85706. Senior Member AIAA.

†Reilly Professor of Engineering, School of Mechanical Engineering and School of Aeronautics and Astronautics, 585 Purdue Mall. Member AIAA.

thrust produced by a single tube. In addition to increasing thrust, multiple-tube engines can be fed from a common inlet and discharged into a common nozzle, thereby reducing the degree of unsteadiness in these components while also providing more favorable matching and improved weight characteristics. One disadvantage of multitube modules, however, is the potential crosstalk that can take place between tubes. Although a valve system can avoid direct interaction through the inlet, the common nozzle provides a direct path for intertube disturbance propagation. The shock wave produced by a detonation from one tube can reflect off adjacent nozzle surfaces and propagate into neighboring tubes. It is this crosstalk aspect of the multitube PDE modules that forms the focus of the present paper. Specifically, two-dimensional analyses are used to study multiple detonation tubes firing into a common nozzle, summarizing previous work on multitube operation [32,33]. The goal is to assess the magnitudes of the disturbances created in adjacent tubes and to identify the degree to which these disturbances can be controlled through geometrical configurations. Ma et al. [34] have recently considered a similar multitube configuration in their more complete inlet/combustor/nozzle analysis [29,30] and report that the precompression in adjacent tubes can modestly enhance performance while the multiple tubes decrease fluctuations. Their results do not indicate any negative impact of intertube crosstalk on the fill process at the single operational point considered (flight Mach number 2.1).

The following sections contain a brief synopsis of the computational model followed by representative comparisons against the experiment to provide validation of the model. This is followed by a series of results for dual and triple tubes exhausting into a common converging–diverging nozzle. As part of parametric studies, the geometry of the splitter plate that separates the individual tubes and their location with respect to the nozzle, as well as the convergence ratio of the nozzle, is varied.

II. Computational Approach and Model Validation

The computational code employed for the present results solves the Navier–Stokes equations by a second-order-accurate explicit/implicit time-marching procedure with second-order upwind discretization in space. Turbulence is incorporated by means of a two-equation turbulence model. Except as noted in the following, the detonation solutions that were used to initiate the shock reverberation calculations in the present paper were based upon an 8-species, 16 reaction, finite-rate kinetic representation of hydrogen and oxygen at stoichiometric conditions. The retention of chemical kinetics allows realistic speeds of sound in both the burned and unburned states of the gas mixture as well as in the external domain, thereby avoiding the somewhat intricate task of defining a global heat release and appropriate averages for the specific heats [19]. Although most PDE models have adopted a "constant-γ" working fluid, similar finite-rate kinetic approaches have been used in several recent PDE studies [25–28,33,35]. In principle, the incorporation of finite-rate chemistry allows resolution of detonation cells, but accurate pressure and temperature jumps can be obtained without cell resolution and would have no impact on the shock reverberation analyses in the present study.

The subject computational code has been previously validated against several steady propulsive flows [36] as well as pulsed detonation engine configurations [31,35]. Grid resolution studies for detonation predictions and comparisons with analytical results and other codes are given in [35], whereas detailed calculation of properties and comparison with experimental data for detonation properties are given in [31]. For example, the predicted detonation speed in a stoichiometric hydrogen/oxygen mixture (2840 m/s) compares favorably with the measured speed (2820 m/s) from an experiment conducted at the same conditions [37]. The close agreement between measured and calculated shock speeds indicates that this detonation model provides an appropriate initial condition for the reverberation calculation.

As a further validation, predictions of the pressure-time history at the head end of a detonation tube are compared with experimental measurements [38] in Fig. 1. The predictions are obtained from a two-dimensional calculation of a PDE tube with a length of 700 mm, which is initially filled with a C_2H_4/air mixture. The comparison between the simulations and the experiments is reasonable, again providing confidence in the simulations as a tool for use in PDE investigations and the ensuing shock reverberations.

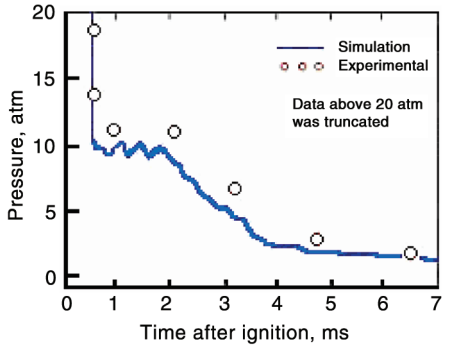

Fig. 1 Comparison of experimental and calculated head-end pressures in a PDE; peak initial value was 30 atm.

III. Geometrical Configurations

Possible geometrical arrangements for multitube PDE modules include a linear array followed by a rectangular nozzle or a cylindrical arrangement that exhausts through an axisymmetric nozzle [3]. Both configurations constitute a complex, three-dimensional geometry. To minimize computational requirements involved in predicting intertube interactions, we consider a two-dimensional system of planar tubes exhausting into a common planar nozzle. The phenomenology described by the two-dimensional configurations provides an initial indication of the full three-dimensional interactions that occur when multiple tubes are combined in this fashion as well as the degree of control available through geometrical modifications, although the quantitative features clearly will be different. Three-dimensional domains allow disturbances to decay more rapidly, but three-dimensional relief should be minimal in these constricted, internal geometries.

Geometrical configurations involving both dual- and triple-detonation tubes exhausting through a common nozzle into an external environment are considered. In both geometries, detonation is initiated in one of the tubes at time zero by filling a short region near the head end of the tube with reaction products at elevated temperature and pressure (3000 K and 30 atm). The remainder of the tube is filled with premixed hydrogen and oxygen in stoichiometric proportion at ambient (300 K and 1 atm) conditions. The nozzle, the external domain outside the system, and the additional detonation tubes in the problem are filled with air at 300 K and 1 atm. The fluid in the entire domain was quiescent at the start of each calculation. A sketch of the initial conditions in a representative, dual-tube geometry is given in Fig. 2.

A Cartesian grid with uniform axial spacing of 0.25 mm is used inside the tubes and the nozzle. The cross-stream spacing in the center of the tubes was similar to the axial spacing, with modestly finer grid near the walls, and is commensurate with that used

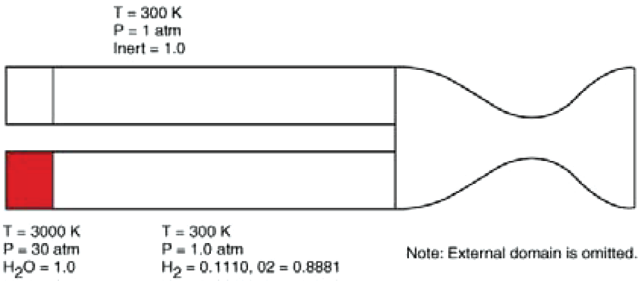

Fig. 2 Initial conditions showing the detonation region in the lower tube of a dual-tube configuration.

elsewhere [24,29] for PDE analyses. Gradual stretching was used in the external domain to a relatively coarse farfield grid in the upstream, downstream, and lateral directions. The initiation region was placed adjacent to the head end of the tube as Fig. 2 suggests and extended over a length of 20 mm, a length similar to that used by Li and Kailasanath [24] but somewhat longer than that reported by Wu et al. [29].

For computational efficiency in this survey of the effect of internal geometry on intertube crosstalk, the analysis uses single-pulse rather than periodic solutions. As in computational performance predictions, multicycle simulations that have reached periodicity are preferable [30,32], but the first-pulse results are expected to be qualitatively representative [14] of intertube crosstalk. Single-pulse analyses continue to serve as the backbone for the PDE studies cited in the preceding text with the exception of [23,29–31,34]. The present multitube optimization analyses serve as a precursor for understanding the flowfield behavior in a multitube/common nozzle system and for developing a strategy for implementing repetitively pulsed multitube computations. Initial multipulse simulations in similar geometries are given elsewhere [34]; however, the limitations of the planar simulations used both here and in [34] should be noted.

IV. Simulations of Dual-Tube Configurations

The basic character of the interactions between detonation tubes in multitube configurations is best understood by starting from a dual-tube configuration. As a detonation exits one tube, a portion of the ensuing shock propagates through the nozzle while the remainder refracts around the splitter plate between the tubes and enters the adjacent tube. Thus, the common nozzle causes a reverse flow to occur in the adjacent tube and increases the pressure level during some portions of the cycle. The details of this reverberation process clearly depend upon the intertube geometry. As specific examples, we consider the two configurations shown in Fig. 3. For both geometries, the detonation tubes are closed on the left end and terminated on the right by a common converging–diverging nozzle. In the first, the nozzle spans both tubes with the entrance to the convergence section beginning at the end of the splitter plate between the tubes, thus creating a constant-detonation tube area throughout the entire tube length. In the second, the splitter plate extends to the throat. Two variations with the splitter plate extending to the nozzle throat were considered. In the one shown here, the nozzle area was equal to the tube area, introducing a short converging section near the exit of the two tubes. In the other, the nozzle area was enlarged to twice that of the tubes so that the areas of the tubes remained constant, although they encountered some curvature. In both computations, when a detonation is introduced into the lower tube it is followed closely by reverberations in the detonated tube, as well as by reverberations induced in the "quiescent" tube.

The dimensions of the detonation tubes were 10 mm in height with an intertube spacing of one-half a tube height (5 mm). Two different tube lengths, 100 and 300 mm, were considered. The tube length controls both the time at which the refracted waves in adjacent tubes hit the head end and the details of the reverberation characteristics. The short tube minimizes the computational time and allows a more economical study of qualitative features. The longer tube simulations were used to estimate how tube length affects the interaction between tubes, and to assess possible tuning effects between tubes and the nozzle. The common converging–diverging nozzle was composed of a second-derivative continuous cubic contour whose convergent section was two tube heights (20 mm) downstream of the constant-area section. As noted in the preceding text, two different throat sizes were used for the dual tubes: one tube height (10 mm) and two tube heights (20 mm). We first present results for the shorter (100-mm) tubes, starting with the dual tubes, and then present dual-tube results for the longer (300-mm) configuration

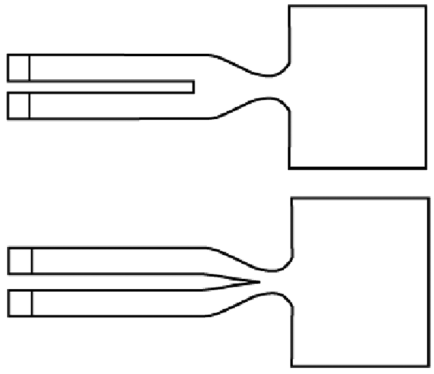

Fig. 3 Representative sketches showing dual-tube geometries including detonation tube, converging–diverging nozzle, and external domain.

A. Pressure Contours for Splitter Plate Terminated at Entrance to Convergent Section

As an initial case, we consider the dual-tube geometry in the top sketch of Fig. 3. Both detonation tubes for this case are of a constant area. The splitter plate ends at the entrance to the convergent part of the nozzle, and the throat is two tube heights downstream of the tube exit with a throat height equal to the tube height (10 mm). Mach number and pressure contours at six different times are shown in Fig. 4 for this case. In the top frame (0.035 ms after initiation) the detonation has just emerged from the lower tube, and the portion of the shock on the upper surface of the tube has begun to expand around the splitter plate, thus bringing fluid into the upper tube while the lower half of the shock is being compressed by the converging section of the nozzle. Because the shock in this frame has not yet hit the upper wall, the results resemble the external shock created by a detonation from an isolated tube except for the containment by the nozzle surface.

In the second frame of Fig. 4 (0.045 ms), the shock has propagated to the upper wall of the nozzle and shows considerable asymmetry in the divergent section. The curvature from the refraction around the splitter plate is still visible inside the upper tube, and the forward-

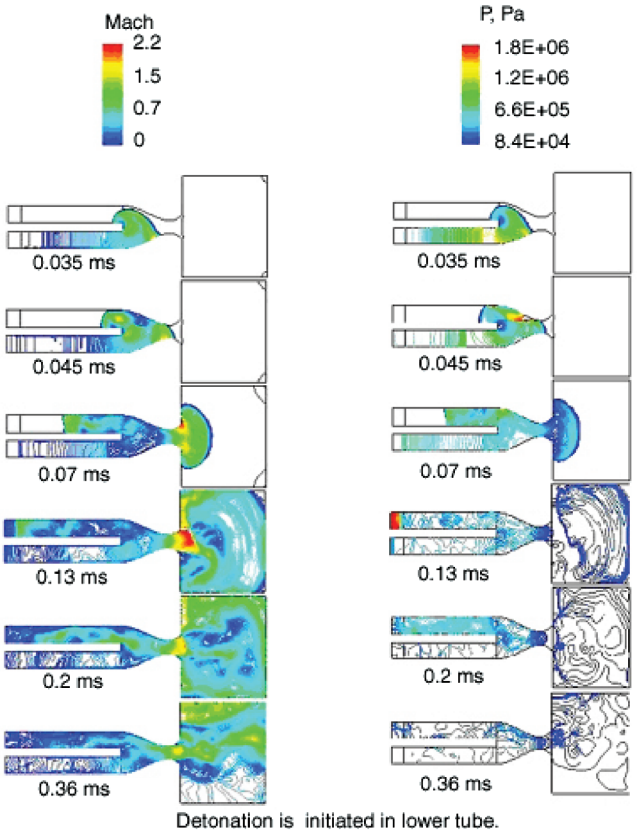

Fig. 4 Time history of pressure and Mach number contours for dual-tube PDE for geometry where splitter plate ends at entrance to the nozzle.

moving shock now covers the entire tube area. In the third frame of Fig. 4 (0.07 ms), the shock in the upper tube has traversed about 70% of the tube and is approaching a planar normal shock. The flow through the divergent section remains asymmetric with a considerable amount of supersonic flow. The highest Mach number is on the upper side of the nozzle, where the expansion is slightly behind that of the lower side.

The shock reflection from the closed end of the upper tube occurs between the third and fourth frames of Fig. 4 and creates a local pressure rise approximately equal to that originally used to initiate the detonation. Nearly all two-dimensional effects have disappeared from the shock by the time it reflects, but refraction effects from the curved section of the nozzle introduce notable two-dimensional effects into the reverberations in the lower tube. The pressure on the upstream wall of the upper tube in the fifth frame is the same magnitude as that produced by the detonation in the lower tube at the corresponding time from initiation. Quantitative details are given in the following line plots. Results for longer tube lengths (shown in the last section) indicate that the strength of the shock reflection off the end wall of the nondetonated tube is somewhat overstated for this relatively short tube.

In the final plot of Fig. 4 (0.36 ms), the pressure on the upstream end of the upper tube has decayed considerably, but remains substantially above ambient conditions. The results suggest that the lower tube may equilibrate to ambient conditions before the upper tube, a situation that may impact the fill process and detonation initiation in the upper tube. It is worthwhile to attempt to modify the geometry to minimize interactions between the tubes. The following section looks at the effect of extending the length of the splitter plate to the nozzle throat.

B. Pressure Contours for Splitter Plate Extended to Throat

The preceding results show that a detonation in the lower tube induces a large overpressure in the upper tube. To assess the degree to which the strength of this refracted wave can be controlled, the effect of changing the geometrical details of the intertube splitter plate is examined. The splitter plate is extended from the entrance to the throat of the convergent section as shown in the lower sketch of Fig. 3. Geometries with two different common throat areas are considered as delineated in Fig. 5. In the plots on the left, the throat is kept the same (10 mm) as that used in the previous dual-tube results, but because the throat area is equal to the tube area, the tubes in this configuration have a convergent section before the open end. For the second geometrical variation, the throat height was increased to twice the tube height (20 mm) so that the areas of both tubes remain constant to the throat although both encounter a slight curvature. This geometry is shown on the right side in Fig. 5. Note that the increased splitter plate length in these cases increases the effective tube length and causes the shock to enter the upper tube at a later time than that for the case given in Fig. 4.

Figure 5 shows pressure contour plots at five different times for both geometries with the splitter plate extending to the throat. The uppermost frame of Fig. 5 corresponds to the time just after the detonation has emerged from the lower tube (0.05 ms). The convergence at the ends of the individual tubes in the geometry on the left causes an internal reflection in the lower tube that is not present in the one at the right and results in a higher pressure near the exit of the tube in the results on the left as compared with those on the right. Also note that the external shock is more highly asymmetric in the larger throat case.

The second pair of frames in Fig. 5 shows conditions at 0.1 ms after initiation. The solutions show that the longer splitter plate delays the shock in the upper tube as compared with the results in Fig. 4, but the results are otherwise qualitatively similar. However, because of the reflection from the convergence at the tube exit that is noted in the preceding, the pressure in the lower tube of the small throat area case on the left is considerably higher than that for the large tube case. This pressure perturbation is thus a "single"-tube phenomenon created by the internal geometry of the lower tube. Note also that there are considerable differences in the expansion process outside the

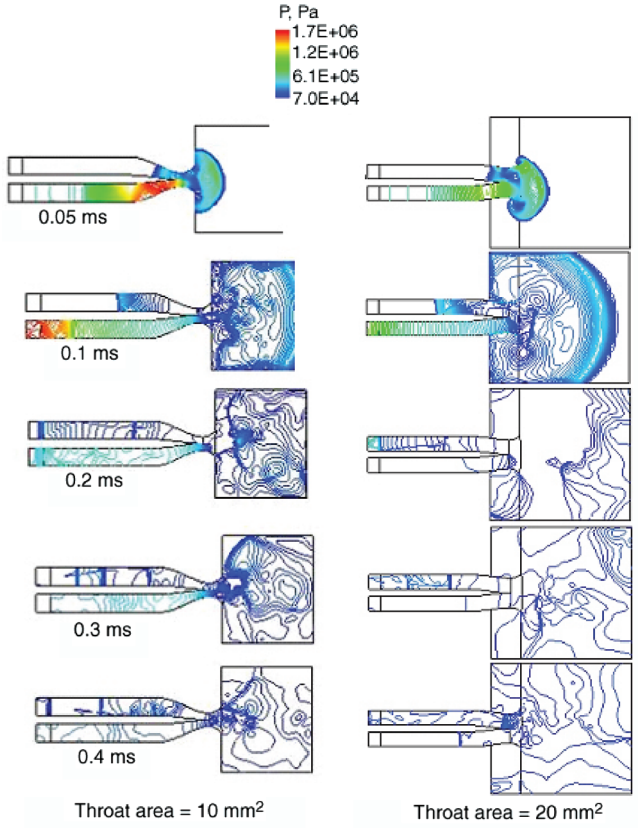

Fig. 5 Comparisons of pressure contours for a dual-tube configuration with splitter plate extended to throat.

common nozzle because of the different throat sizes and the differing tube-end geometries. The pressure in the nozzle is considerably lower for the larger throat area configuration. Corresponding Mach number contours [32] similarly show that, in general, the larger throat size results in smaller supersonic regions.

The pressure contours at the three remaining times (0.2, 0.3, and 0.4 ms) demonstrate that extending the splitter to the throat has a major impact on the strength of the reflected shock in the upper tube. Extending the splitter plate to the throat allows the effects of the initial pulse to pass through the throat more readily and reduces the interactions between the two tubes substantially. Increasing the throat height allows the pressure in both the lower and upper tubes to decay more rapidly than it does for the smaller throat case.

C. Time History in Dual-Tube Calculations

To provide more quantitative interpretations of the preceding computations, in Fig. 6 we have presented time histories of the pressure at the midpoint of the head ends of both the upper and lower tubes for all three configurations. Case 1 corresponds to the geometry of Fig. 4, where the splitter ends at the entrance to the convergent section. Case 4 corresponds to results in the left half of Fig. 5, where the splitter is extended to the throat. Case 3 corresponds to an intermediate case, where the splitter extends halfway into the convergent section [33]. All cases have the same 10-mm throat height. The lower plot depicts the pressure in the lower tube, and the upper plot depicts the pressure in the upper tube.

For all three cases the pressure in the lower tube starts with a strong 30-atm spike that corresponds to the pressure used for the numerical detonation initiation. As the detonation propagates through the lower tube, the pressure on the lower end wall decreases to the P3 pressure, where it remains until a reflection from the open end arrives. Cases 3 and 4 first experience a reflection from the convergent section at the end of the tube. This reflection results in an increase in the pressure at the head end. Case 1, which has a constant-area tube, first receives an expansion wave from the open end of the tube; this is followed by a weak compression from the convergent section of the nozzle. Cases 3

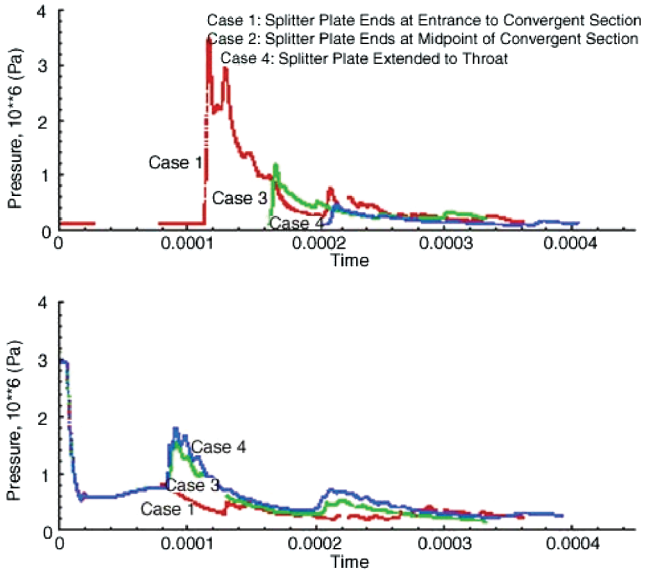

Fig. 6 Comparison of pressure histories on head end of upper (top) and lower (bottom) tube showing the effect of intertube geometry on the strength of reflected shock.

and 4, both of which have a converging section at the end of the tube, first show a compression arising from waves off this convergent section; they then show an expansion when the wave reaches the open end.

The end-wall pressures in the top tube remain at ambient conditions until the detonation in the lower tube has reached the splitter plate, refracted around it, and traversed back up the upper tube. The time required for the reflection to reach the head end of the upper tube is increased as the splitter plate length is increased from case 1 to case 3 to case 4 because of the longer effective length of the tubes. However, the rate of decay of the pressure spike in all cases is quite rapid because the arriving shock is followed by a sequence of rarefaction waves.

The most obvious observation from the upper plot in Fig. 6 is that the strength of the reflection is strongly dependent on the splitter plate length. In case 1, the reflected wave in the upper tube is almost equal to the detonation initiation pulse in the lower tube. The strength of this wave is dramatically reduced by extending the splitter plate into the nozzle. For case 3, the peak of the reflected wave is approximately one-third that of case 1, whereas for case 4, where the splitter extends to the throat, the pressure peak is decreased by approximately a factor of 6. Thus, it is clear that careful design can have a major effect on the strength of the reflected wave. The overpressure for case 4 is, however, still approximately 4 atm. The reflected pressure peak in the adjacent tube is also decreased somewhat as the tube length is increased, as is shown in a following section.

Additional computations with the splitter extended into the divergent portion of the nozzle showed no additional decrease in the strength of the reflected wave and actually led to a modest increase in the pressure peak, suggesting that ending the splitter at the throat results in approximately a minimum pressure peak. In addition to the splitter plate location, the size of the throat of the common nozzle has an effect, albeit a lesser one, on the strength of the initial reflection and its rate of decay [24].

V. Triple-Tube Configuration Simulations

The geometry for the triple-tube configuration is shown in Fig. 7. It included three tubes of constant area with both splitter plates ending at the beginning of the convergent section in a fashion identical to that used for the results in Fig. 4. The tube dimensions were again 10 mm high by 100 mm long, with an intertube spacing of 5 mm. The throat height was 22.5 mm. For all calculations, a large, unconfined region was placed outside the diverging section to account for external perturbations. For the triple-tube geometry, the detonation

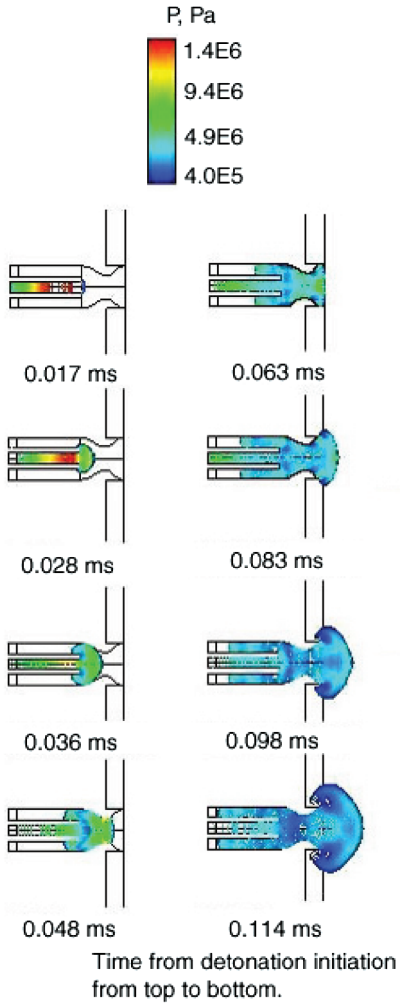

Fig. 7 Time history of pressure contours for the triple-tube case with splitter plate terminated at the entrance to the convergent section.

was initiated in the central tube so that the ensuing reverberation of the pulse in all three tubes and the converging–diverging nozzle could be observed. Some results for additional geometries of this family are given in [32,33].

The pressure contours for this triple-tube case are presented in Fig. 7 for eight time intervals. The upper-right plot in the figure corresponds to the time (0.036 ms) after the detonation has emerged from the middle tube and is just reaching the nozzle walls. Up to the time shown in this plot, the solution is identical to that for an isolated tube. The contours remain completely symmetric as the shock diffracts around the splitter plates on either side of the central tube and the flow is starting to enter the upper and lower tubes. Simultaneously, the shock wave is propagating into the converging section of the nozzle.

The second, third, and fourth plots in Fig. 7 correspond to 0.028 to 0.48 ms after the detonation initiation. At this time, the shock has entered the upper and lower tubes and is approximately halfway through the divergent section of the nozzle. The succeeding plots show the propagation of the shock toward the head end of the upper and lower tubes and the corresponding pressure reverberations in the middle tube. The symmetric geometry eliminates any asymmetries but gives an estimate of the impact of expansions into multiple tubes on the pressure impact at the head end.

Line plots comparing the pressure histories on the head ends of the dual- and triple-tube configurations are given in Fig. 8 to show the degree to which the reflected shock in the adjacent tubes is changed in the triple-tube case as compared with the dual-tube case. As in Fig. 6, results are given for both the “driver” and the “driven” tubes, this time in a single plot. The early time results for the tube containing the detonation are identical for both the dual- and triple-tube cases

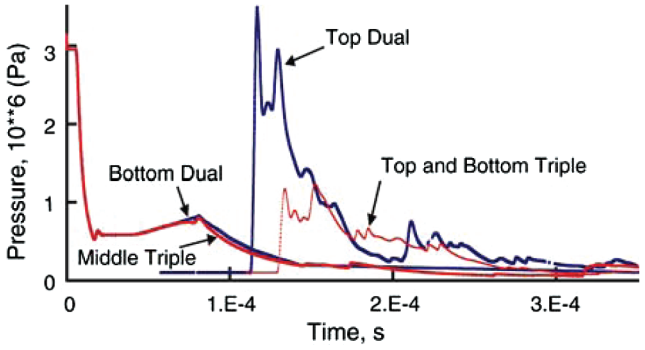

Fig. 8 Comparison of pressure-time histories on head-end walls for dual- and triple-tube configurations with splitter plate terminated at the entrance to the convergent section.

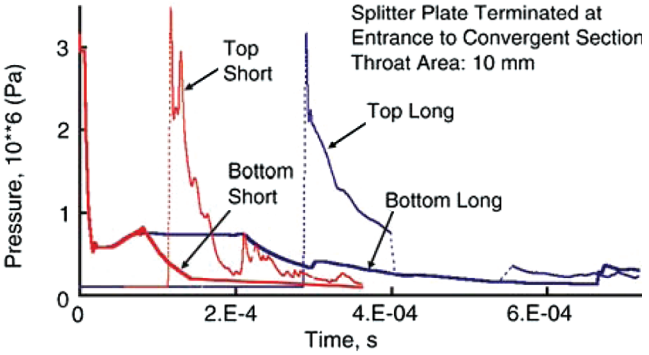

Fig. 10 Comparison of time histories of pressure on upper and lower end walls for the short and long tubes.

because the geometries are identical and the traces begin to differ only as effects of the downstream configuration are propagated back into the flowfield. The primary observation of this comparison is that the reflected wave in the triple-tube case is reduced by more than a factor of 2 compared with that for the dual-tube case. This difference arises because of the expansion into two tubes in the triple-tube case rather than one in the dual-tube case, coupled with the focusing provided by the adjacent convergent section in the dual-tube case that strengthens the reflection in the upper tube.

VI. Effect of Tube Length

In the preceding subsections we have shown the effects of changes in the number of tubes and the intertube geometry on the reverberations in adjacent tubes. Here the effects of changing the tube length from 100 to 300 mm are summarized. Here attention is limited to the dual-tube case and the manner in which the splitter plate length impacts the reflected waves. We begin by comparing the pressure contours in a dual-tube configuration that is identical to that presented in Fig. 4 except for its increased length. Specifically, the splitter plate is terminated at the entrance to the convergent section of the nozzle, the throat height is 10 mm, and the intertube spacing is 5 mm.

Pressure contours for this 300-mm tube with three different time intervals are given in Fig. 9. The results are qualitatively the same as for the shorter tube. The first set of contours for the long tube on the upper plot of Fig. 9 shows the pressure 0.065 ms after initiation, just as the detonation is emerging from the lower tube. This condition is chosen to match the similar plot in Fig. 6. As for the short-tube case, the contours exhibit strong two-dimensionality as the shock wave diffracts around the splitter plate, causing the flow to enter the upper tube. Apart from the difference in the time taken for the detonation to reach the end of the tube (because of the difference in tube length), local conditions near the splitter plate are identical in the two calculations.

The middle plot in Fig. 9 illustrates the continued propagation of the shock into the upper tube at a time of 0.101 ms and is to be compared with the shorter tube results in the second plot in Fig. 6.

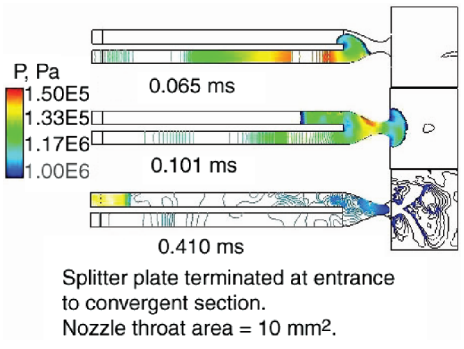

Fig. 9 Time history of pressure contours for a 300-mm tube.

Again, the flow is similar to conditions in the shorter tube, but it is no longer identical because tube length effects have begun to appear. As the tube length is increased, expansion waves overtake and weaken the shock before it reflects from the head end, causing the magnitude of the reflected pressure to be reduced.

At the third time interval, 0.410 ms, the shock in the upper tube has reflected from the head end, and conditions in the upper tube are roughly analogous to those in the third plot of Fig. 6. Overall, the comparison between the two tube lengths shows qualitatively similar flow characteristics. The key issue is to compare the strengths of the reflected waves in the adjacent tube in a quantitative sense.

The time histories of the pressure on the end wall of both the lower and upper tubes is given in Fig. 10 for both the long and short tubes. The lighter curve is for the shorter tube, whereas the darker curve is for the longer tube. Again, the most obvious difference between the two tube lengths occurs because of the substantial time difference between events, but a more detailed inspection provides additional insight. Looking first at the early-time results, one can see that the head-end pressure history in the lower tube is identical for both tube lengths until the first reflection from the open end of the shorter tube reaches the head end. At that time the pressure in the shorter tube begins to depart from that for the longer tube, and the reverberation processes in the longer tube start taking place on a longer timescale. When comparing the pressure peaks generated by the refracted wave in the upper tube, one can see that although the magnitude of the reflected wave in the upper tube is only slightly affected by the added length, it nevertheless is reduced somewhat. The rate of decay is also a bit slower, again reflecting the longer characteristic time of the longer tube. Clearly, the configuration with the splitter plate ending before the convergent section engenders very strong reflections into the adjacent tube. As noted in the preceding, this pressure peak is substantially affected by the reflected shock's expansion into multiple side tubes, but in all cases the reflected waves are strong.

Similar comparisons of the pressure history on the head end of the long and short tubes when the splitter geometry is extended to the

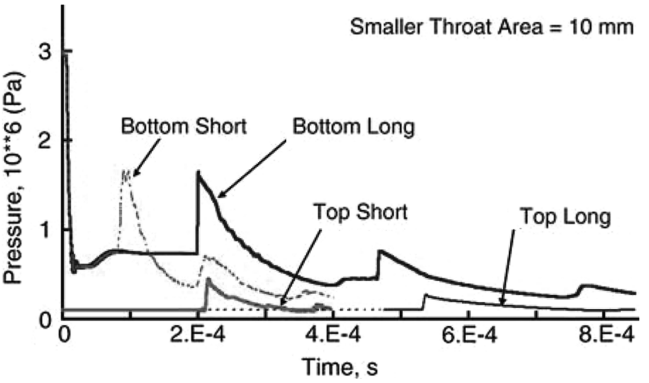

Fig. 11 Comparison of time histories of pressure on upper and lower end walls for the short and long tubes with splitter plate extended to throat.

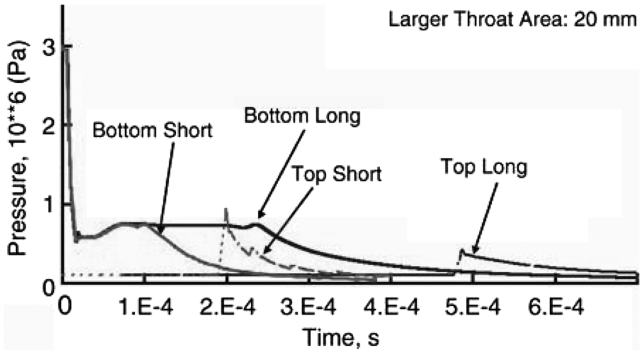

Fig. 12 Comparison of time histories of pressure on upper and lower end walls for the short and long tubes with splitter plate extended to throat.

nozzle throat are given in Figs. 11 and 12. Figure 11 presents results for the smaller throat area (10 mm) analogous to the geometry in the left half of Fig. 5, where the tubes have a convergent section before they exit into the nozzle. Figure 12 is for the larger throat area (20-mm) geometry, analogous to that shown on the right in Fig. 5. In both cases, the effect of increasing the tube length results in a decrease in the reflected pressure level in the adjacent tube. The results in Fig. 11 for the smaller throat area case show that the peak pressure in the adjacent tube is reduced from 4.4 to 3.1 atm. For the larger throat area case, the pressure peak is reduced from 9.7 to 4.3 atm. The passage convergence in the smaller throat area case of Fig. 11 generates a compression that is clearly visible on the head end of the lower tube in both the long- and short-tube cases, whereas the constant-area passages in Fig. 12 give more conventional traces in the lower tubes.

The results of all the geometrical variations on the peak pressure level in the adjacent tube(s) are summarized in Table 1. The peak pressure reached in the adjacent tube changes by an order of magnitude for the geometrical variations described herein. In general, extending the end of the splitter plate toward the throat or increasing the tube length decreases the strength of the reflected pressure perturbation, as does adding a third tube. The pressure appears to increase for the larger throat area case, but the larger throat area also appears to be more sensitive to the tube length than the smaller throat does. The substantial variation in the magnitude with which a given change affects the peak pressure from one condition to another suggests that detailed wave characteristics and interactions have considerable impact on these induced pressures. Additional analyses of specific geometries is necessary to identify an absolute minimum pressure perturbation in adjacent tubes, but the present results suggest that careful design can provide substantial dividends.

VII. Summary and Conclusions

The characteristics of internal reverberations in multitube PDEs have been investigated by means of a two-dimensional computational model. The class of geometries considered is composed of dual- and triple-planar detonation tubes exhausting into a common nozzle. The focus has been on identifying the level of interaction and crosstalk between adjacent detonation tubes and the degree to which the interaction can be controlled by geometrical variations.

The results show that the pressure induced in one tube by the detonation from a neighboring tube can be as large as that produced by the original detonation. Shocks of this magnitude are strong enough to initiate combustion prematurely in adjacent tubes, if they are filled with fresh propellants, or to adversely impact filling if the fill valves are open. The likelihood of premature combustion increases as more tubes are added to an engine module. The magnitude of this reverberation can, however, be reduced by nearly a factor of 10 by modifying the intertube geometry through extending the splitter plate to the nozzle throat, changing the nozzle throat area, or increasing the number of adjacent tubes. Careful analysis of the unsteady flowfields is needed to ensure proper operation of multitube PDE systems.

Table 1 Reflected peak pressures in adjacent tubes

Configuration	Length, mm	Splitter plate[a]	Throat area	Pressure, atm
Dual tube	100	Conv	10	35
Dual tube	100	Conv	10	31
Triple tube	100	Conv	22.5	12.5
Dual tube	100	Half	10	12.1
Dual tube	100	Throat	10	4.4
Dual tube	300	Throat	10	3.1
Dual tube	100	Throat	20	9.7
Dual tube	300	Throat	20	4.3

[a]Splitter plate configurations denote length of splitter: Conv: Terminated at entrance to convergent area. Half: Extends halfway through convergent area. Throat: Extends to throat.

Acknowledgments

The research reported herein was performed by the Arnold Engineering Development Center (AEDC), Air Force Materiel Command. Work and analysis for this research were performed by personnel of Purdue University and by personnel of Aerospace Testing Alliance, the operations, maintenance, information management, and support contractor for AEDC. Further reproduction is authorized to satisfy needs of the U.S. Government.

References

[1] Nicholls, J. A., Wilkinson, H. K., and Morrison, R. B., "Intermittent Detonation as a Thrust-Producing Mechanism," *Jet Propulsion*, Vol. 27, No. 5, 1957, pp. 534–541.

[2] Eidelman, S., Grossmann, W., and Lottati, I., "Review of Propulsion Applications and Numerical Simulations of the Pulse Detonation Engine Concept," *Journal of Propulsion and Power*, Vol. 7, No. 6, 1991, pp. 857–865.

[3] Bussing, T. R. A., and Pappas, G., *Pulse Detonation Engine Theory and Concepts*, Progress in Astronautics and Aeronautics Series, edited by S. N. B. Murthy and E. T. Curran, Vol. 165, AIAA, Reston, VA, 1996, pp. 421–472.

[4] Zitoun, R., and Desbourdes, D., "Propulsive Performances of Pulsed Detonations," *Combustion Science and Technology*, Vol. 21, No. 2, 2005, pp. 274–285.

[5] Brophy, C. M., and Netzer, D., "Effects of Ignition Characteristics and Geometry on the Performance of a JP-10/O2 Fueled Pulse Detonation Engine," AIAA Paper 99-2635, June 1999.

[6] Schauer, F., Stutrud, J., and Bradley, R., "Detonation Initiation Studies and Performance Results for Pulsed Detonation Engines," AIAA Paper 2001-1129, Jan. 2001.

[7] Cooper, M., Jackson, S., Austin, J., Wintenberger, E., and Shepherd, J. E., "Direct Experimental Impulse Measurements for Deflagrations and Detonations," *Journal of Propulsion and Power*, Vol. 18, No. 5, 2002, pp. 1033–1041.

[8] Austin, J. M., and Shepherd, J. E., "Detonations in Hydrocarbon Fuel Blends," *Combustion and Flame*, Vol. 132, 2003, pp. 73–90. doi:10.1016/S0010-2180(02)00422-4

[9] Kailasanath, K., "Review of Propulsion Applications of Detonation Waves," *AIAA Journal*, Vol. 38, No. 9, 2000, pp. 1698–1708.

[10] Kailasanath, K., "Recent Developments in Research on Pulse Detonation Engines," *AIAA Journal*, Vol. 41, No. 2, 2003, pp. 145–159.

[11] Mattison, D. W., Brophy, C. M., Sanders, S. T., Ma, L., Hinckley, K. M., Jeffries, J. B., and Hanson, R. K., "Pulse Detonation Engine Characterization and Control Using Tunable Diode-Laser Sensors," *Journal of Propulsion and Power*, Vol. 19, No. 4, 2003, pp. 568–572.

[12] Radulescu, M. I., and Hanson, R. K., "Effect of Heat Loss on Pulse-Detonation-Engine Flow Fields and Performance," *Journal of Propulsion and Power*, Vol. 21, No. 2, 2005, pp. 274–285.

[13] Frolov, S. M., Basevich, V. Y., Aksenov, V. S., and Polikhov, S. A., "Spray Detonation Initiation by Controlled Triggering of Electric Dischargers," *Journal of Propulsion and Power*, Vol. 21, No. 1, 2005, pp. 54–64.

[14] Cooper, M., and Shepherd, J. E., "Detonation Tube Impulse in Subatmospheric Environments," *Journal of Propulsion and Power*, Vol. 22, No. 4, 2006, pp. 845–851.

[15] Schauer, F. R., Miser, C. L., Tucker, K. C., Bradley, R. P., and Hoke, J. L., "Detonation Initiation of Hydrocarbon-Air Mixtures in a Pulsed

Detonation Engine," AIAA Paper 2005-1343, Jan. 2005.
[16] Heiser, W. H., and Pratt, D. T., "Thermodynamic Cycle Analysis of Pulse Detonation Engines," *Journal of Propulsion and Power*, Vol. 18, No. 1, 2002, pp. 68–76.
[17] Kentfield, J. A. C., "Fundamentals of Idealized Airbreathing Pulse-Detonation Engines," *Journal of Propulsion and Power*, Vol. 18, No. 1, 2002, pp. 77–83.
[18] Talley, D., and Coy, E., "Constant Volume Limit of Pulsed Propulsion for a Constant Gamma Ideal Gas," *Journal of Propulsion and Power*, Vol. 18, No. 2, 2002, pp. 400–406.
[19] Wintenberger, E., Austin, J. M., Cooper, M., Jackson, S., and Shepherd, J. E., "Analytical Model for the Impulse of Single-Cycle Pulse Detonation Tube," *Journal of Propulsion and Power*, Vol. 19, No. 1, 2003, pp. 22–38.
[20] Wintenberger, E., and Shepherd, J. E., "Model for the Performance of Airbreathing Pulse-Detonation Engines," *Journal of Propulsion and Power*, Vol. 22, No. 3, 2006, pp. 593–603.
[21] Wintenberger, E., and Shepherd, J. E., "Stagnation Hugoniot Analysis for Steady Combustion Waves in Propulsion Systems," *Journal of Propulsion and Power*, Vol. 22, No. 4, 2006, pp. 835–843.
[22] Zel'dovich, Y. B., "To the Question of Energy Use of Detonation Combustion," *Journal of Propulsion and Power*, Vol. 22, No. 3, 2006, pp. 588–582.
[23] Cambier, J.-L., and Tegner, J. K., "Strategies for Pulsed Detonation Engine Performance Optimization," *Journal of Propulsion and Power*, Vol. 14, No. 4, 1998, pp. 489–498.
[24] Li, C., and Kailasanath, K., "Partial Fuel Filling in Pulse Detonation Engines," *Journal of Propulsion and Power*, Vol. 19, No. 5, 2003, pp. 908–916.
[25] Fan, H. Y., and Lu, F. K., "Comparison of Detonation Processes in a Variable Cross-Sectional Chamber and a Simple Tube," *Journal of Propulsion and Power*, Vol. 21, No. 1, 2005, pp. 65–75.
[26] Morris, C. J., "Numerical Modeling of Single-Pulse Gasdynamics and Performance of Pulse Detonation Rocket Engines," *Journal of Propulsion and Power*, Vol. 21, No. 3, 2005, pp. 527–538.
[27] He, X., and Karagozian, A. R., "Pulse-Detonation-Engine Simulations with Alternative Geometries and Reaction Kinetics," *Journal of Propulsion and Power*, Vol. 22, No. 4, 2006, pp. 852–861.
[28] Perkins, H. D., and Sung, C.-J., "Effects of Fuel Distribution on Detonation Tube Performance," *Journal of Propulsion and Power*, Vol. 21, No. 3, 2005, pp. 539–545.
[29] Wu, Y., Ma, F., and Yang, V., "System Performance and Thermodynamic Cycle Analysis of Airbreathing Pulse Detonation Engines," *Journal of Propulsion and Power*, Vol. 19, No. 4, 2003, pp. 556–567.
[30] Ma, F., Choi, J.-Y., and Yang, V., "Thrust Chamber Dynamics and Propulsive Performance of Single-Tube Pulse Detonation Engines," *Journal of Propulsion and Power*, Vol. 21, No. 3, 2005, pp. 512–526.
[31] Ebrahimi, H. B., Mohanraj, R., and Merkle, C. L., "Multi-Level Analysis of Pulsed Detonation Engines," *Journal of Propulsion and Power*, Vol. 18, No. 2, April 2002, pp. 225–232.
[32] Ebrahimi, H. B., and Merkle, C. L., "Optimization of Multi-Tube Pulse Detonation Configuration," AIAA Paper 2002-4228, July 2002.
[33] Ebrahimi, H. B., and Merkle, C. L., "Numerical Investigations of Multi-Tube Pulse Detonation Engines," AIAA Paper 2003-1035, Jan. 2003.
[34] Ma, F., Choi, J.-Y., and Yang, V., "Thrust Chamber Dynamics and Propulsive Performance of Multitube Pulse Detonation Engines," *Journal of Propulsion and Power*, Vol. 21, No. 4, 2005, pp. 681–691.
[35] Ebrahimi, H. B., "Numerical Simulation of Transient Jet-Interaction Phenomenology in a Supersonic Freestream," *Journal of Spacecraft and Rockets*, Vol. 37, No. 6, Dec. 2000, pp. 713–719.
[36] Ebrahimi, H. B., and Merkle, C. L., "A Numerical Simulation of the Pulse Detonation Engine with Hydrogen Fuels," *Journal of Propulsion and Power*, Vol. 18, Oct. 2002, pp. 1042–1048.
[37] Soloukhin, R. I., *Shock Waves and Detonations in Gases*, Mono Book, Baltimore, MD, 1966.
[38] JANNAF Combustion, Airbreathing Propulsion, Propulsion Systems Hazards, and Modeling and Simulation Subcommittees 4444–4450, 2000.

V. Yang
Associate Editor